JOURNAL OF GEOPHYSICAL RESEARCH, VOL. ???, XXXX, DOI:10.1029/,

Wind-profiler observations of gravity waves produced by convection at mid-latitudes

Y. G. Choi,[1] S. C. Lee,[2] and A. J. McDonald[3]

Department of Physics and Astronomy, University of Canterbury, Private Bag 4800, Christchurch, New Zealand.

[1]Geophysical Prospecting Laboratory, Seoul National University, Korea.

[2]Department of Physics, Kangnung National University, Korea

[3]Department of Physics and Astronomy, University of Canterbury, Private Bag 4800, Christchurch, New Zealand.

Abstract. This study presents two case studies which include regions of large rapidly varying vertical velocities observed by a VHF wind-profiler at Aberystwyth (52.4° N, 4.1° W). Analysis indicates that both these regions are associated with gravity waves above the tropopause level and simultaneous regions of convective activity are identified below the tropopause level. Convective activity is identified by finding periods associated with large uncertainties on the derived velocities which in turn are hypothesized to be related to regions of small-scale inhomogeneity in the wind field. The presence of convection is also confirmed by near-simultaneous satellite imagery that shows evidence of convective clouds in the vicinity of Aberystwyth during the case studies.

Examination suggests that the large vertical velocity fluctuations above these convective regions are short period gravity wave packets. The appearance of short period gravity waves directly above the convective source region is as expected from theory. In addition the vertical momentum flux associated with the gravity waves also displays the pattern of reversal observed in previous studies.

1. Introduction

Convection and gravity waves associated with convection have previously been observed at tropical latitudes by wind-profilers, aircraft, satellites and radiosondes. For example, *Dhaka et al.* [2002] discuss observations of convection made by the Indian MST radar and gravity waves which are suggested to be generated by the convection. *Vincent et al.* [2004] also discuss observations of gravity waves made by a wind profiler data during the DAWEX experiment which are shown to be highly likely to be generated by convection. *Alexander et al.* [2000] used wind measurements from the ER2 aircraft in the stratosphere to obtain information on the momentum flux carried by gravity waves. Their study compared the cloud top brightness temperature below the aircraft, which is assumed to be an indicator of deep convective activity, with momentum flux data taken by the ER2 aircraft during the STEP project. Their work indicated a striking correlation between cold, high clouds and large wave momentum flux. *Dewan et al.* [1998] explained concentric circles observed in satellite data as gravity waves originating from isolated thunderstorms. *Karoly and Reeder* [1996] examined gravity wave activity associated with tropical convection detected in TOGA COARE sounding data.

Observations of convective activity have also recently been observed at mid-latitudes [*Hooper et al.*, 2005]. As indicated in *Hooper et al.* [2005] a number of different signals are generally observed during periods of atmospheric convection, these include large rapidly varying vertical velocities, large values of vertical spectral width and occasionally enhanced signal powers in the upper troposphere. The aim of this study is to show two case studies where convection has been identified as the probable cause of enhanced gravity wave activity and compare these measurements with previous observations and theory.

There are generally three mechanisms discussed to explain the generation of gravity waves by convection. One is the 'topographic effect' where convection cells act as temporary obstacles in the atmosphere when the background wind has significant vertical shear waves can be produced upstream(?this is what it states in the beres paper?) of the obstacle. The second is the 'mechanical oscillator' when oscillating updrafts and downdrafts impinge on the tropopause (or possibly other stable layers) and short-period gravity waves are excited. The third and the most commonly examined is the effect associated with latent heat release and the thermal forcing of waves [*Beres et al.*, 2002].

It should be noted that while this work is the first in our knowledge to focus on mid-latitude convection observed by ST radar, work described in *Vincent et al.* [2004] has shown some similar features associated with tropical convection. Similar results have also been indicated in *Dhaka et al.* [2002]. In addition another recent study at mid-latitudes has indicated a region of convection and examined the potential of convective mixing for exchanging air between the boundary layer and a region associated with a tropopause fold [*Reid and Vaughan*, 2004]. That study confirms that the convection interacts with the tropopause level and perhaps produces a subsequent mixing of stratospheric and tropospheric air.

Sato et al. [1995] also indicates that convection is known to be an important source of gravity wave generation. Observations described in *Sato et al.* [1995] show enhanced vertical velocities in one case up to the tropopause level. However, the magnitude of these is much smaller than observed in *Hooper et al.* [2005] and was not associated with precipitation. Their study also suggests that an observation shows wave generation from cumulus convection and possible absorbtion later at a critical layer.

Vertically propagating gravity waves generated by convection are known to provide an important contribution to the momentum budget of the middle atmosphere. Thus, understanding the wave field observed at higher altitudes relative to particular convective sources has also been studied. For example, gravity wave theory predicts that isolated, sufficiently convective thunderstorms can launch waves and create a unique intensity pattern of concentric circles on a radiating surface of constant altitude above such a storm. This was confirmed by *Dewan et al.* [1998] which presents evidence that certain of the 4.3micron images of atmospheric emissions obtained from the MSX satellite show structures that are due to gravity waves originating from isolated thunderstorms. Meteorological satellite images being used to show that highly convective isolated thunderstorms occurred at the locations and times of the expected generation zones.

Horinouchi and Kosaka [2002] discuss a 3-dimensional simulation which utilised a cloud-resolving model to investigate mesoscale gravity waves generated by cumulus convection that propagates to the mesospheric and lower thermospheric (MLT) region. Both individual turrets and mesoscale convective systems excite gravity waves, resulting in a broad scale of parameters for the gravity waves excited by convection. Their simulation excited waves produced by individual turrets and these waves had conically shaped phase surfaces as reported previously by *Dewan et al.* [1998] and are conspicuous up to the stratopause. *Horinouchi and Kosaka* [2002] suggests that waves excited by MCS's are thought to dominate in the MLT.

Nakamura and Suranto [2003] display OH airglow imaging observations carried out over Indonesia which show 74 gravity wave events in the MLT. Observed period, horizontal wavelength and horizontal phase speeds were 5-13 mins, 13-45km, and 37-75m/s, respectively. Propagation directions were southward except for the period between December and February, when eastward propagation was preferential. Spatial distributions of tropospheric cloud were consistent with the propagation direction of the gravity waves. This suggests that horizontal propagation characteristics of short period gravity waves in the MLT are affected by the distribution of wave sources in the troposphere, rather than the effect of the background wind. This is suggested to be associated with the weaker winds in the equatorial region.

2. Method

The NERC MST radar at Aberystwyth (52.4°N, 4.1°W), described in *Vaughan* [2002], operates at a frequency of 46.5 MHz and has a peak transmitted power of 160 kW. The antenna consists of a 20 by 20 array of four element Yagi aerials covering an area of 110 m by 110 m. The radar beam has a one-way half-power half-width of 1.5 degrees and it can be steered in sixteen possible directions. These include the vertical and at angles of 4.2, 6.0, 8.5 and 12.0 degrees off-vertical in a variety of azimuths.

This radar derives parameters from Doppler spectra using a simple, single-peak spectral processing technique. The mean noise power spectral density (PSD) is evaluated using the objective algorithm of *Hildebrand and Sekhon* [1974]. The spectral limits of the signal are bound by those points at which the PSD, to either side of the peak PSD, first drops below the mean noise PSD. For strong signals, the limits are further restricted by identifying those points at which the PSD first drops to 0.01 of the peak PSD. The principal spectral parameters of signal power, Doppler shift and spectral width are then calculated within these limits by the standard method described by *Woodman* [1985]. In this study, zonal and meridional components of wind have been derived using beams at 6 degrees off-vertical in azimuths parallel to the diagonals of the array and in the zenith direction; measurements using two pairs of ± 6 degree directions have also been used to derive estimates of momentum flux. In the present study for each radar cycle, observations were made twice in the vertical direction and once each in the SW6, NW6, NE6 and SE6 directions. This oversampling of the wind field allows the least squares technique used to derive confidence intervals on the wind measurements, described in *Astin* [1997], to be utilized.

3. Results

This study examines two days in which periods of strong convective activity have been observed in VHF wind-profiler data. In particular, a specific case study, using observations from 1st March 2003, which clearly displays a period of deep convection that reaches the tropopause level is discussed. A second case study, using observations from 4th May 2002, which displays shallower convection is also detailed. Examination of both dates suggests large vertical velocity perturbations are also observed above the tropopause. Significantly above the tropopause level the vertical velocity perturbations observed are unlikely to be associated with convective regions. It is proposed that these perturbations are associated with internal gravity waves produced by convection. The possibility that the enhanced vertical velocities are associated with Mountain wave activity which displays a similar signature [*Prichard et al.*, 1995; *Rottger*, 2000] is also explored.

3.1. Case study: 1st March 2003

Observations of the mean vertical profiles of the zonal and meridional velocities averaged over 1st March 2003 are displayed in Figure 1. In each case the spread of values at each altitude, as represented by the standard deviation, is also displayed. Examination of Figure 1 (a) shows that the mean zonal wind remains westerly at all altitudes. The variation of the mean zonal wind is from 10 m/s to 20 m/s with a maximum around 9.5 km this maximum is associated with the edge of a jet which is located approximately 200km to the south of Aberystwyth. The mean meridional wind displayed in Figure 1 (b) is southerly up to 16 km altitude and again has a maximum close to 9.5km. The mean tropopause altitude, identified using the radar signal power structure using a method similar to that discussed in *Larsen and Rottger* [1983], is located at 8.3 km which is below the wind maximum. Close examination of the zonal and meridional velocity profiles above 12 km also displays clear fluctuations with a vertical wavelength of approximately 1.2km which examination suggests are associated with inertia gravity waves. However, it is important to note that this gravity wave is not considered to be associated with the convection.

Figure 2 displays time series of the vertical velocity at a range of altitudes between 2 and 16km. To ensure only good velocity estimates are utilized the velocity data related to low signal strengths and regions where poor temporal continuity is observed are interpolated over by applying an 8th order polynomial fitting along height. Large vertical velocity fluctuations are observed between approximately 12:30 and 13:30UT in Figure 2. At lower altitudes, between 1.7 and 9km, between 13:00 and 14:00UT a large updraft with a maximum magnitude of 7.4ms^{-1} is also observed. The updraft is followed by a downdraft which is dominant up to approximately 4.5km altitude. Above 4.5km the updraft continues to be the dominant structure up to the tropopause level. The vertical velocities above the tropopause are also enhanced in this period. However, examination suggests that the average magnitude of the vertical velocities is much smaller and that the vertical velocities show clear periodic wave-like structure. In Figure 2 the tropopause level is defined using the radar signal power structure using a method similar to that discussed in *Larsen and Rottger* [1983]. Use of a tropopause sharpness criterion allows the quality of the tropopause altitude estimate to be tested. Examination suggests that the tropopause is poorly defined in the region directly above the convective region. It is possible that this poor definition may be associated with the mixing of stratospheric and tropospheric air at the top of the convective region. Observations discussed in *Reid and Vaughan* [2004] display clear evidence of the impact that convection can have on stratosphere-troposphere exchange processes. It is also possible that any gravity waves produced by the convection could also affect cause mixing around the tropopause level (Pavelin, ???).

In addition to the structure identified below the tropopause level, several wave-like fluctuations are observed in the vertical velocity field which propagate well above the tropopause altitude. These wave-like structures which are observed to have very short periods, 30 minutes or below, seem likely to be triggered locally by the convective region. It is interesting to note that another region of large vertical velocity activity is also observed around 14:00UT. However, this regions vertical extent is more limited and the vertical velocity variance is not as great as observed at 12:30 to 13:30UT.

It should be noted that the fact that short period gravity waves are observed directly above convection is to be expected based on theoretical considerations [*Beres et al.*, 2002;

Alexander and Holton, 2004]. In fact *Alexander and Holton* [2004] indicates that the locally observed response to a convective heat source depends strongly on the distance of the observer from the source. In particular, an observer (or wind profiler) close to the source will see long vertical wavelength waves with high frequencies lasting for a short time, while further from the source the dominant vertical wavelength would be smaller and frequency lower, the waves would arrive later, and they would persist longer. This result can be understood by noting that the ratio of wave frequency to buoyancy frequency determines the angle to the vertical at which the wave propagates. This is also general to all the forcing mechanisms and thus this observation dos not allow us to determine the type of generation mechanism. Their theoretical work also suggests that the wave observed therefore also only makes up a small portion of the wave field generated. However, the short period gravity waves observed in this case are likely to be of considerable importance because of the large momentum flux associated with these waves [*Nayar and Sreeletha*, 2003; *Sato*, 1990].

Ancillary information from satellite and radiosonde soundings suggests that the interpretation of the large vertical velocity fluctuations in the troposphere as convective signatures is valid. However, a number of authors [*Prichard et al.*, 1995; *Rottger*, 2000] have indicated that large vertical velocity perturbations are also produced by mountain waves. To examine the plausibility of the large vertical velocities being associated with mountain waves Figure 3 displays the hourly averages of vertical velocity, along with profiles of the low-level background wind speed and direction. The low-level wind speed and direction was determined from wind-profiler data averaged over the lowest height gates of the radar(i.e. 1.7-2.7km). The directions shown in Figure 3 are those from which the wind is blowing, in degrees clockwise from north. For convenience, the vector diagram of low-level wind is also shown on the lowest panel of Figure 3. Simultaneous measurements of large mean vertical velocities and low-level wind directions over mountainous terrain are a good indicator of mountain wave activity. Examination of the low-level data indicates that during the period of largest vertical velocities the wind speed varies little and that the direction remains close to the SW direction. *Prichard et al.* [1995] indicates that at Aberystwyth the topography between the NNW and SW direction is less than 150 m height for several kilometres. Thus, the wind direction is such that the wind is unlikely to produce significant mountain-wave activity. The fact that wind direction and speed remain relatively unchanged from 06:00 to 18:00UT and the lack of a corresponding increase in the vertical velocity throughout this period also suggests that the observations are unrelated to mountain wave activity.

It is still possible that changes in the static stability of the atmosphere during this period could produce this pattern. However, mesoscale temperature structure data from the UK Met Office Unified model [*Cullen*, 1993; *Lopez et al.*, 2003] does not suggest that the static stability of the atmosphere changes significantly in this period (see Figure 4). Comparison of the vertical signal power, displayed in Figure 4 (a), with the temperature structure data suggests that the tropopause level derived from the UK Met Office model data corresponds very well to an enhancement in the vertical signal power observed. The tropopause altitudes identified by both methods were located at heights between 7 and 9 km. The signature of the tropopause in the signal power can be attributed to the greater static stability of the stratosphere relative to the troposphere [*Larsen and Rottger*, 1983]. In addition the vertical signal power data displayed in Figure 4 (a) shows a clear enhancement around 13:00UT between 4 and 8km. This enhancement could be due to a number of factors, but is one of the signatures of mid-latitude convection identified in *Hooper et al.* [2005]. However, it is worth indicating that enhanced radar return signal power is the least commonly observed signature of convection and that *Hooper et al.* [2005] indicates that this is likely to be associated with the fact that this signature is only likely to be present when a strong contrast in humidity exists between the in-cloud and surrounding air. Careful comparison of the vertical signal power data with the vertical velocity data, shown in Figure 2 (a), suggests that the region of vertical velocity enhancement displays a much greater altitudinal extent than the vertical signal power enhancement. This fact seems to suggest that the vertical velocity enhancements above and below this level have a different character. This leads to the interpretation of large vertical velocities relating to a convective region up to the tropopause level overlaid by a region of enhanced vertical velocities which are more periodic in nature which are potentially high frequency internal gravity waves.

A time-altitude contour plot of the beam-broadening corrected spectral width is displayed in Figure 4 (b). The clearest feature in this contour plot is a region of large corrected spectral widths which are coincident with the enhancement in the vertical signal power previously discussed above. *Hooper et al.* [2005] indicates that large values of the corrected spectral width also constitute one of the signatures of convection observed by VHF radar. Under normal conditions the value of the corrected spectral width can be used as a measure of turbulent intensity. However, it should be noted that the interpretation of spectral width is not obvious during periods of significant rainfall [*Chu and Lin*, 1994]. Surface rainfall data measured by an ARG tipping bucket rain gauge suggests particularly heavy precipitation at approximately 13:20UT (not shown). Thus, it is not possible to identify this region as strong turbulence. However, this feature again is consistent with the interpretation of this region as convection.

Figure 5 displays time-altitude contour plots of the zonal, meridional and vertical velocities and their corresponding confidence intervals for 1st March 2003. The confidence intervals on the velocities have been derived using the method described in *Astin* [1997]. Briefly, this method uses a least squares approach based on the geometry of the beam positions and a set of radial velocity measurements to determine the velocities in the cardinal directions and their confidence intervals. The confidence intervals are used in this study because large values can be used to indicate where the underlying assumption of local homogeneity used in the Doppler Beam Swinging method is no longer valid. *Vincent et al.* [2004] notes the absence of wind measurements during times when convection is strong. Their work suggests that these gaps may be associated with convection. Any convective cells passing over the radar produced strong small-scale variations in winds, causing spectral broadening of the echoes. Correspondingly, the correlation functions used in the spaced antenna full correlation analysis (FCA) are narrow, and the analysis often breaks down. Thus, we can use the uncertainties to identify the regions associated with convection. *Vincent et al.* [2004] indicates that the horizontal scale necessary to produce such a heterogeneous wind field would be unlikely to be produced by gravity waves. Thus, this method also allows the possibility of separating regions of large vertical velocities associated with convection and gravity waves. Examination of Figure 5 indicates large uncertainties in both the horizontal and vertical winds during the 12:30 to 13:30UT between 2 nd 10km. It is suggested that this is associated with the lack of local homogeneity in the wind-field which would be observed in a convective cell. Careful inspection also suggests that this lack of inhomogeneity is not observed to such a great degree above the tropopause level. Further suggesting that there is a fundamental difference between the vertical velocity perturbations below and above the tropopause level. We believe that this suggests that the large vertical velocities in the troposphere are associated with convection and those above the tropopause are related to wave packets of short-period internal gravity waves.

Based on the assumption indicated above we have applied a spectral approach to examine whether the periodic fluctuations in the vertical velocity field are more abundant above the convective region and to determine their dominant periodicity. The method utilized applies a Fast Fourier Transform algorithm to the vertical velocities in a 90 minute segment and shifts the central time of the segment from the start to the end of the time series available which covers a 24 hour period. This method is repeated at altitudes between 12 and 16 km, the individual frequency spectra from the 90-minute segments are then averaged together to form a set of representative frequency spectra. Figure 6 displays the power spectral density as a function of the time of the central value used in the spectra for periods ranging between 90 and 5 minutes. Examination of Figure 6 suggests a number of regions where peaks in the power spectral density are observed. The upper altitude of the height range used was chosen because the highest altitude which contains reliable vertical velocities without the need to interpolate the data lies on average at roughly 17km. The lower altitude used in the altitude range was selected in order to exclude the effect of the convective region itself. After summing the spectral powers between the chosen altitudes we obtain Figure 6. The increase of the spectral power around the convection region indicates there are periodic fluctuations around this region, which coincide with the above hypothesis. Inspection suggests periods between 5 and 45 minutes are enhanced during the convective period.

The enhancement in the power spectral density observed in Figure 6 can also be observed in an alternative form by calculating the mean vertical velocity variance as a function of time. The mean vertical velocity variance calculated using approximately 1 hour averages over the altitude range 12 to 16km is displayed in Figure 7. Figure 7 displays data for the unfiltered vertical velocity variance and bandpass filtered vertical velocity variance data. The bandpass filters used have two distinct lower and upper limits, one is between 6 and 60 minutes and the other is between 1 and 3 hours, respectively. Examination of the bandpass filtered data up to 60 minutes shows a distinct enhancement in activity at around 13:30UT, corresponding exactly to the convective period observed below the tropopause level. The bandpass filtered data of 1 and 3 hours does not show any noticeable enhancement at around this time, but has a sharp peak at around 9:00UT. This means the waves at around 13:30UT have only short periods below 1 hour and the periods of waves at around 9:00UT are distributed widely up to 3 hours. This result is expected given that similar enhancements at short periods at around 13:30UT and longer periods at around 9:00UT have been observed in Figure 6. Examination of the unfiltered data shows the surprising result that an enhanced vertical velocity square is observed between approximately 08:00 and 15:00UT. Comparison of this period with the low-level wind speed and direction in Figure 3 suggests that this enhancement could be associated with mountain wave activity. This is a little surprising given the low altitude terrain passed over which would not be expected to produce significant wave activity. However, the existence of gravity waves at longer periods around 09:00UT is also observed in Figure 6 and thus this wide distribution of unfiltered data is due to the mixing of gravity waves of longer periods at earlier times and shorter periods at later time.

The time variation of the vertical fluxes of horizontal momentum above the tropopause level has been calculated using data from two pairs of oppositely directed radar beams which are directed 6 degrees off the vertical zenith angle. Two methods have been applied to determine the momentum flux, the first is the symmetric-beam radar method discussed by *Vincent and Reid* [1983], the other is the power spectra method detailed in *Sato* [1990]. The momentum flux has been calculated for 90 minute periods of data and averaged across 1.5km. It should be noted that because the two methods are based on a statistical method, many data points are needed to minimize the statistical fluctuations. In an attempt to remove the effect of the inertia gravity wave previously discussed and displayed in Figure 2 we have applied a band-pass filter to the velocities when using the *Vincent and Reid* [1983] method and have summed only data with selected frequencies between 6 and 45 minutes in the case of the *Sato* [1990] method. It should be noted that contrary to the suggestion in *Nayar and Sreeletha* [2003] little difference between the values derived by these two methods is discernible. The results from the *Sato* [1990] method are shown in Figure 8. The calculation of the momentum flux is made between 12.7 and 14.2km well above the local tropopause level. Below the tropopause level, very large momentum fluxes around the convection region are observed. However, it should be noted that these momentum fluxes will have very large uncertianties because of the large uncertianties of the component velocities (see Figure 5). In addition, it should be noted that this analysis is not discussed for observations below the tropopause level because of the difficultly of separating any gravity wave perturbations from the convective activity. *Vincent et al.* [2004] notes this problem with this type of study.

Examination of the momentum flux data above the tropopause level, displayed in Figure 8 suggests that a region of enhanced momentum flux is observed during the convective period. Close inspection also indicates that the momentum flux vector changes direction from northward to southward between 13:00 and 14:00UT. A similar sign change in momentum flux calculations has previously been observed using ER2 aircraft observations by *Alexander et al.* [2000] during periods associated with convective gravity waves. The vertical flux of horizontal momentum thus also shows evidence of the existence of gravity waves related to convection. The increase of the magnitude of momentum flux and its change of sign also suggest that there should be waves propagating around this region.

3.2. Case study: 4th May 2002

The second case study presented again shows signs of convective activity and related gravity wave activity. However, in this case the magnitude of the gravity wave activity is much reduced compared to that observed in the previous case study. Figure 9 displays time series of the vertical velocity at a range of altitudes between 2 and 16km. Large vertical velocity fluctuations are observed at two periods, these being around 01:00UT and between approximately 10:30 and 14:30UT in Figure 9. Both sets of variations extend from 2 to 4km and are suggested to be shallow convection. This is confirmed by large uncertainties on the velocity measurements derived using the method indicated in *Astin* [1997] as previously used in section 3.1. Examination of the vertical velocity field directly above the second region also indicates enhanced vertical velocities between 7 and 14km. Though these are not as large as those observed in the previous case study. It should be noted that a low pass filtered version of the data using a bandpass of 3 hours shows a more defined version of this diagram and again indicates that the internal gravity wave field observed is dominated at this time by short-period gravity waves.

Figure 10 displays the mean vertical velocity variance between 10 and 13.9km. It should be noted that the lower limit was selected because the radar data suggests that the tropopause altitude is at roughly 9km throughout the day and the value therefore represents the vertical velocity variance in the lower stratosphere. Examination of the vertical velocity variance associated with filtered and unfiltered data indicates a clear variation withe maxima at 01:00, 12:00 and 21:00 UT. It is suggested that the first two of these maxima are related to increased gravity wave activity again associated with the shallow convection. This is similar to the result observed on 1st March 2003 but much less clear. In particular it should be noted that the vertical velocity variances associated with these two convective events are smaller than those observed on 1st March 2003 by a factor of 5 or more. In addition comparison of the vertical velocity variance for the periods 1 to 3hours and 6 to 60 minutes again suggests that the wave field is dominated by shorter period waves.

4. Conclusions and Further work

It has been suggested that by examining the uncertainties on velocity data, derived using the method indicated in *Astin* [1997], it may be possible to identify periods of active convection. This interpretation of this data leads to the analysis of the large vertical velocity perturbations observed in both case studies as periods of convection overlaid by short-period gravity waves. Simulations by *Alexander and Holton* [2004] indicate that the locally observed response to a convective heat source depends strongly on the distance of the observer from the source. In particular their suggestion that an observer close to the source will see long vertical wavelength waves with high frequencies lasting for a short time seems to be validated by this study. However, this correspondence does not suggest that the mechanism used to force the gravity waves in the observations is the same as that indicated in *Alexander and Holton* [2004] since all the mechanisms used to generate gravity waves from convection would produce similar patterns with respect to the source region. However, the fact that the first case study (1st March 2003) also displays a momentum flux field that changes direction during the period of enhanced gravity wave activity seems to prohibit the 'topographic effect' in this case since this mechanism is suggested to produce waves that propagate preferentially opposite to the background wind direction [*Beres et al.*, 2002]. The 'topographic effect' occurs when convective cells act as temporary obstacles in the atmosphere. Thus, no change in direction around the time of the convection would be expected since this pattern would be indicative of gravity wave generation that ideally would produce an activity pattern of concentric circles on a surface of constant altitude. In this case, the mechanical oscillator or the thermal forcing mechanisms seem more appropriate. The relative magnitude of the wave field produced in the two case studies suggests that the depth and strength of convection might contribute to the magnitude of the wave produced. But, again does not allow the particular mechanism to be identified.

It is also interesting to note that a number of other convective events have been observed in the radar data and that none of the other events have shown similar patterns perhaps suggesting that both of these events are unusual in the magnitude of the waves observed.

Further work will focus on identifying whether this is true by identifying more convective periods using regions associated with large uncertainties.

Acknowledgments. The MST Radar Facility at Aberystwyth is funded by the UK Natural Environment Research Council and the data presented in this paper has been kindly provided through the British Atmospheric Data Centre. We would also like to thank the (UK) Met Office who kindly provided the UM mesoscale model data to the British Atmospheric Data Centre. We also wish to acknowledge the Dundee Satellite Receiving Station which provided the AVHRR data. Dr. McDonald would like to acknowledge grant U6518 from University of Canterbury. S. C. Lee has been supported by the research foundation of Kangnung National University.

References

Alexander, M. J., and J. R. Holton, On the spectrum of vertically propagating gravity waves generated by a transient heat source, *Atmospheric Chemistry and Physics*, *4*, 923–932, 2004.

Alexander, M. J., J. H. Beres, and L. Pfister, Tropical stratospheric gravity wave activity and relationships to clouds, *J. Geophys. Res.*, *105*, 22,299–22,309, 2000.

Astin, I., Confidence interval estimation for vhf doppler radar measurements of wind velocities, *Radio Science*, *32*(6), 2221–2231, 1997.

Beres, J. H., M. J. Alexander, and J. R. Holton, Effects of tropospheric wind shear on the spectrum of convectively generated gravity waves, *J. Atmos.Sci.*, *59*, 1805–1824, 2002.

Chu, Y.-H., and C.-H. Lin, The severe depletion of turbulent echo power in precipitation observed using the Chung-Li VHF Doppler radar, *Radio Science*, (29), 1311–1320, 1994.

Cullen, M. J. P., The unified forecast climate model, *Meteorological Magazine*, *122*(1449), 81–94, 1993.

Dewan, E. M., R. H. Picard, R. R. O'Neil, H. A. Gardiner, G. J., J. D. Mill, E. Richards, M. Kendra, and W. O. Gallery, Msx satellite observations of thunderstorms-generated gravity waves in mid-wave infrared images of the upper stratosphere, *Geophysical Research Letters*, *25*(7), 939–942, 1998.

Dhaka, S. K., R. K. Choudhary, S. Malik, Y. Shigabaki, M. D. Yamanaka, and S. Fukao, Observable signatures of a convectively generated wave field over the tropics using Indian MST radar at Gadanki (13.5° N, 79.2° E), *Geophys. Res. Let.*, *29*(18), doi: 10.1029/2002GL014745, 2002.

Hildebrand, P. H., and R. S. Sekhon, Objective determination of the noise level in Doppler spectra, *Journal of Applied Meteorology*, *13*, 808–811, 1974.

Hooper, D. H., A. J. McDonald, A. K. Patra, P. B. Rao, G. Viswanathan, and K. Subramanian, Midlatitude convection paper, *Geophys.Res. Lett.*, *???*, ???, 2005.

Horinouchi, N. T., T., and J.-I. Kosaka, Convectively generated mesoscale gravity waves simulated throughout the middle atmosphere, *Geophysical Research Letters*, *29*(21), doi:10.1029/2002GL016,069, 2002.

Karoly, R. G. L., D. J., and M. J. Reeder, Gravity wave activity associated with tropical convection detected in toga coare sounding data, *Geophysical Research Letters*, *23*(3), 261–264, 1996.

Larsen, M. F., and J. Rottger, Comparison of tropopause height and frontal boundary locations based on radar and radiosonde data, *Geophysical Research Letters*, *10*(4), 325–328, 1983.

Lopez, P., K. Finkele, P. Clark, and P. Mascart, Validation and intercomparison of three mesoscale models on three fastex cloud systems: Comparison with coarse-resolution simulations, *Quarterly Journal of the Royal Meteorological Society*, *129*(591), 1841–1871, 2003.

Nakamura, A. T. T. T. A. A. G. A. E., T., and Suranto, Mesospheric gravity waves over a tropical convective region observed by oh airglow imaging in indonesia, *Geophysical Research Letters*, *30*(17), doi: 10.1029/2003GL017,619, 2003.

Nayar, S. R. P., and S. Sreeletha, Momentum flux associated with gravity waves in the low-latitude troposphere, *Annales Geophysicae*, *21*(5), 1183–1195, 2003.

Prichard, I. T., L. Thomas, and R. M. Worthington, The characteristics of mountain waves observed by radar near the west coast of wales, *Annales Geophysicae*, *13*, 757 – 767, 1995.

Reid, H. J., and G. Vaughan, Convective mixing in a tropopause fold, *Quarterly Journal of the Royal Meteorological Society*, *130*(599), 1195–1212, 2004.

Rottger, J., ST radar observations of atmospheric waves over mountainous areas: a review, *Ann. Geophys.*, *18*, 750–765, 2000.

Sato, K., Vertical wind disturbances in the troposphere and lower stratosphere observed by the MU radar, *J. Atmos. Sci.*, *47*, 2803–2817, 1990.

Sato, K., H. Hashiguchi, and S. Fukao, Gravity-waves and turbulence associated with cumulus convection observed with the uhf/vhf clear-air doppler radars, *Journal of Geophysical Research-Atmospheres*, *100*(D4), 7111–7119, 1995.

Vaughan, G., The uk mst radar, *Weather*, *57*(2), 69–73, 2002.

Vincent, R. A., and I. M. Reid, Hf doppler measurements of mesospheric gravity-wave momentum fluxes, *Journal of the Atmospheric Sciences*, *40*(5), 1321–1333, 1983.

Vincent, R. A., A. MacKinnon, I. M. Reid, and M. J. Alexander, Vhf profiler observations of winds and waves in the troposphere during the darwin area wave experiment (dawex), *Journal of Geophysical Research-Atmospheres*, *109*(D20), 2004.

Woodman, R. F., Spectral moment estimation in MST radars, *Radio Science*, *20*, 1185–1195, 1985.

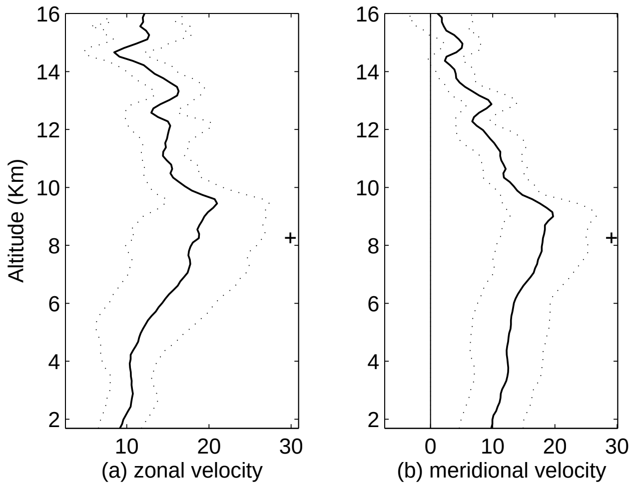

Figure 1. Height profiles of mean meridional and zonal wind speeds for 1st March 2003. The spread of values at each height, as represented by the standard deviation, is shown by dashed lines. Also shown on the right axis is the mean tropopause altitude as derived from MST radar data.

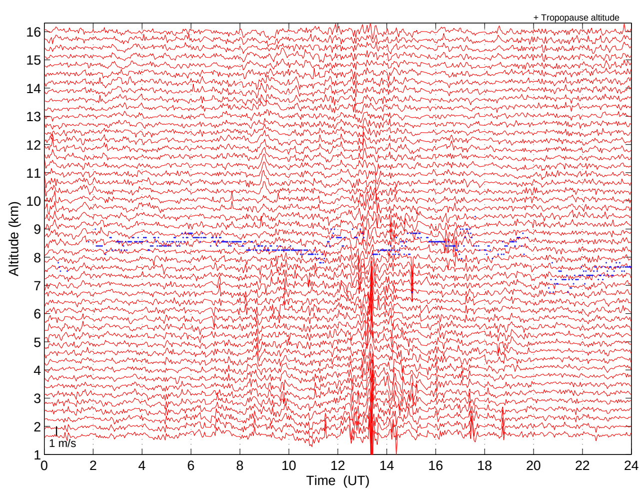

Figure 2. Time series of vertical wind velocity on 1st March 2003 from the first gate (1.7km) to 16km with 0.3km interval along height. The magnitude of vertical velocity is shown along left hand side in m/s. The tropopause altitudes derived from MST radar data are shown by cross points.

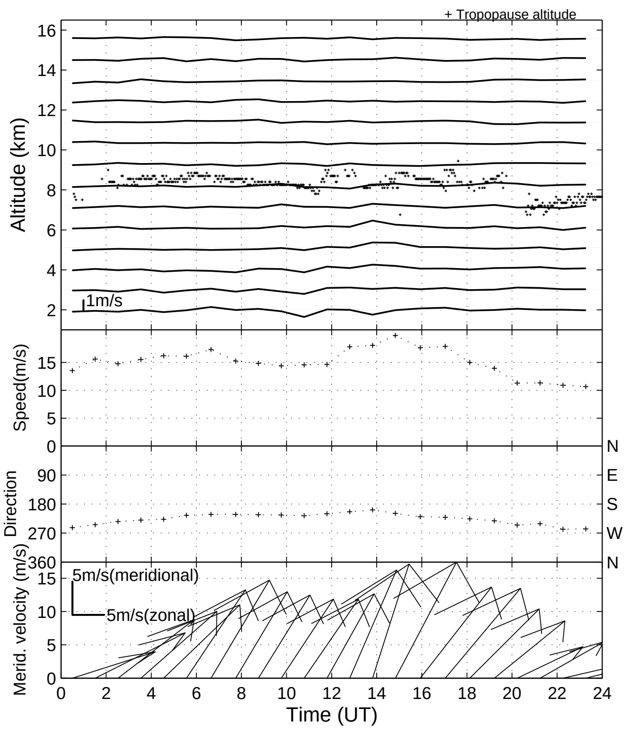

Figure 3. Hourly averages of the vertical velocity and tropopause altitudes and low-level wind speed and direction for 1st March 2003. The upper panel depicts the variations of mean vertical velocity at approximately 1km intervals from 2 to 16km. The tropopause altitueds are shown as Fig. 2. The three lower panels indicate wind speed and direction for the height range 1.7-2.7km directions being those from which the wind blowing, in degrees clockwise from north. And the lowest panel shows the vectors of low-level horizontal winds.

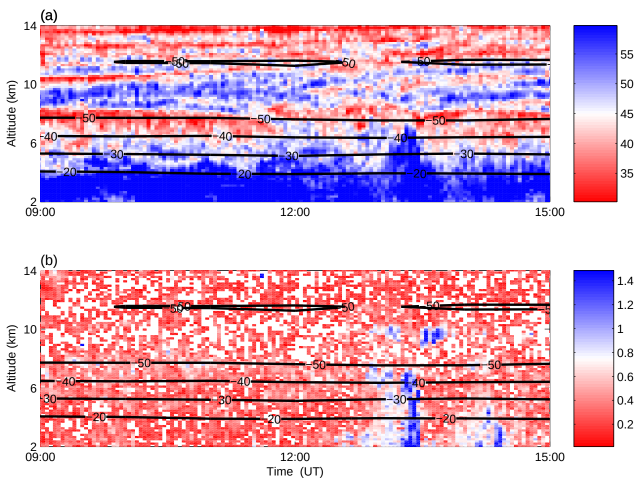

Figure 4. Time-height contour plots of (a) vertical signal power (dB) and (b) corrected spectral width (ms^{-1}) measured by a VHF radar for 09:00 to 15:00UT on 1st March 2003. Overplotted on each time-height plot are temperature contours obtained from UK Met Office mesoscale Unified Model output over Aberystwyth.

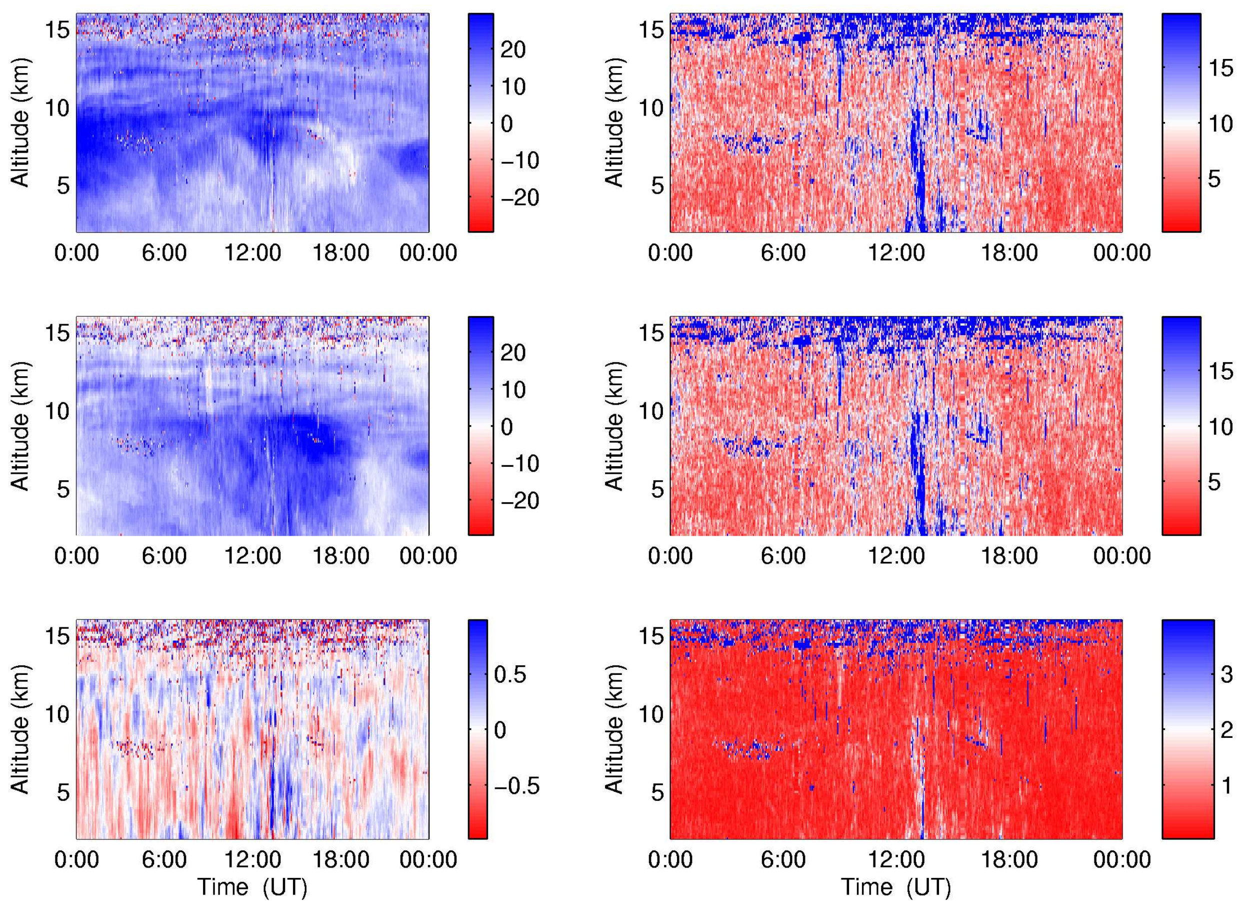

Figure 5. Time-altitude contour plots of the zonal, meridional and vertical velocities and their respective confidence intervals are shown.

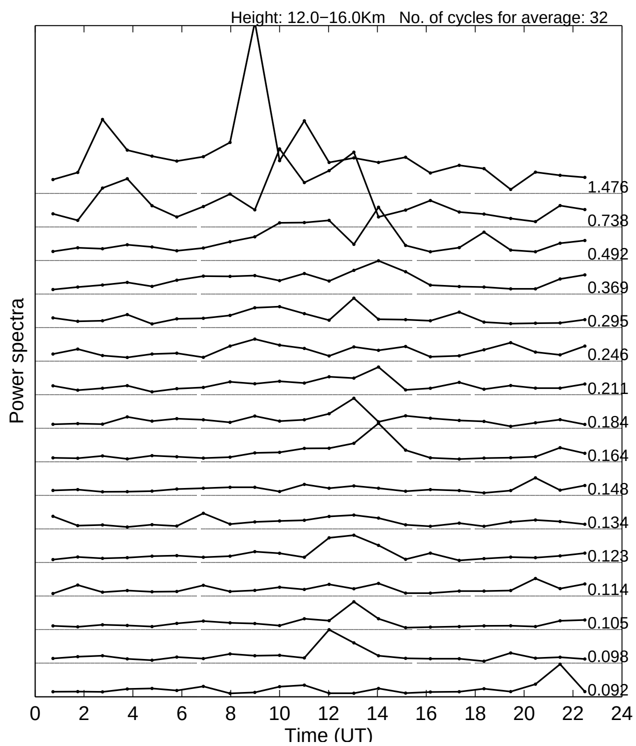

Figure 6. Time-period plots of spectral power of vertical velocities from 12-16km using fast Fourier Transform. Number of time cycles for each FFT calculation per a gate is 32. After the time segment is fixed, the spectra per each gate within the selected range are calculated. And the sum of spectral power of each period is plotted at every segment. The highest curve represents low frequency (1.5 hour, long period) component along time axis and the lowest curve indicates high frequency (5.5 minutes, short period).

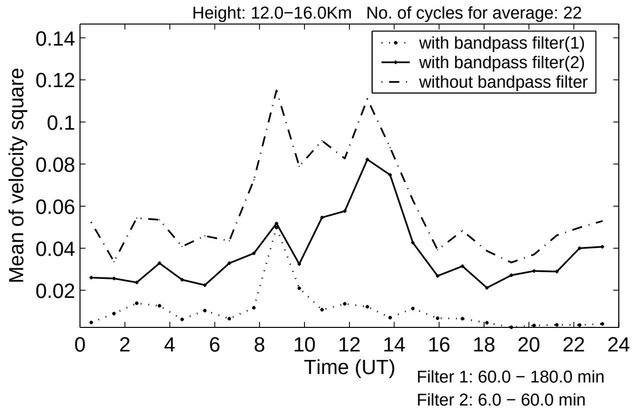

Figure 7. Time-mean vertical velocity square plots using approximately 1 hour averages over the altitude range 12-16km. The mean vertical velocity square without bandpass filter is shown as a dash-dot line. A dotted line is for the mean velocity square calculated after applying a bandpass filter which has lower and upper period limits of 3 and 1 hours, respectively. And the solid line represents the mean square calculated after applying a bandpass filter with shorter periods, lower and upper boundaries of 1 hour and 6 minute. In this shorter period range, the mean vertical velocity square at around 13:00UT has high amplitude.

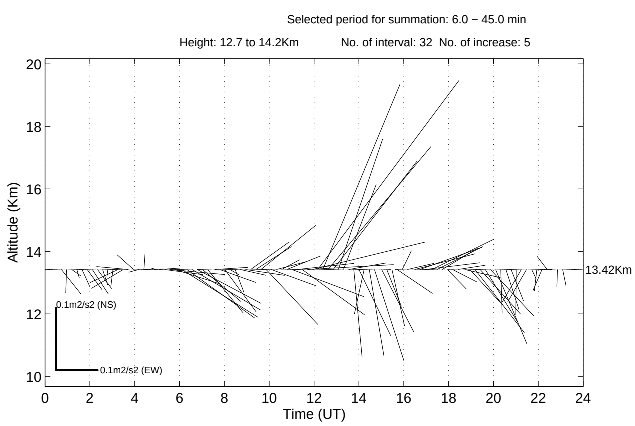

Figure 8. Vector plots of time variation of the vertical flux of horizontal momentum using the power spectra method by Sato on 1st March 2003. The momentum flux are calculated for every segment with 32 time cycles and averaged over altitudes from 12.7 to 14.2km.

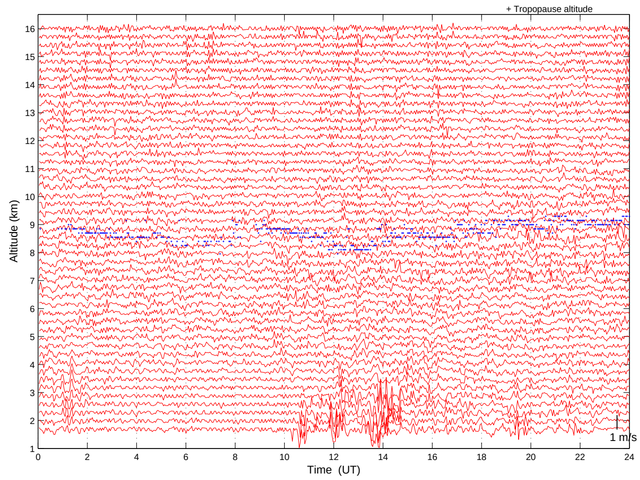

Figure 9. Time series of vertical wind velocity on 4th May 2002 from the first gate (1.7km) to 16km with 0.3km interval along height. The magnitude of vertical velocity is shown along left hand side in m/s. The tropopause altitudes derived from MST radar data are shown by crosses.

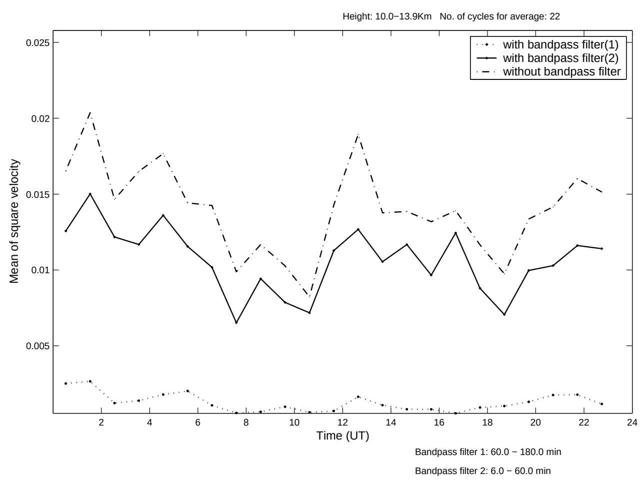

Figure 10. Time-mean vertical velocity square plots using approximately 1 hour averages over the altitude range 12-16km. The mean vertical velocity square without bandpass filter is shown as a dash-dot line. A dotted line is for the mean velocity square calculated after applying a bandpass filter which has lower and upper period limits of 3 and 1 hours, respectively. And the solid line represents the mean square calculated after applying a bandpass filter with shorter periods, lower and upper boundaries of 1 hour and 6 minute. In this shorter period range, the mean vertical velocity square at around 13:00UT has high amplitude.